

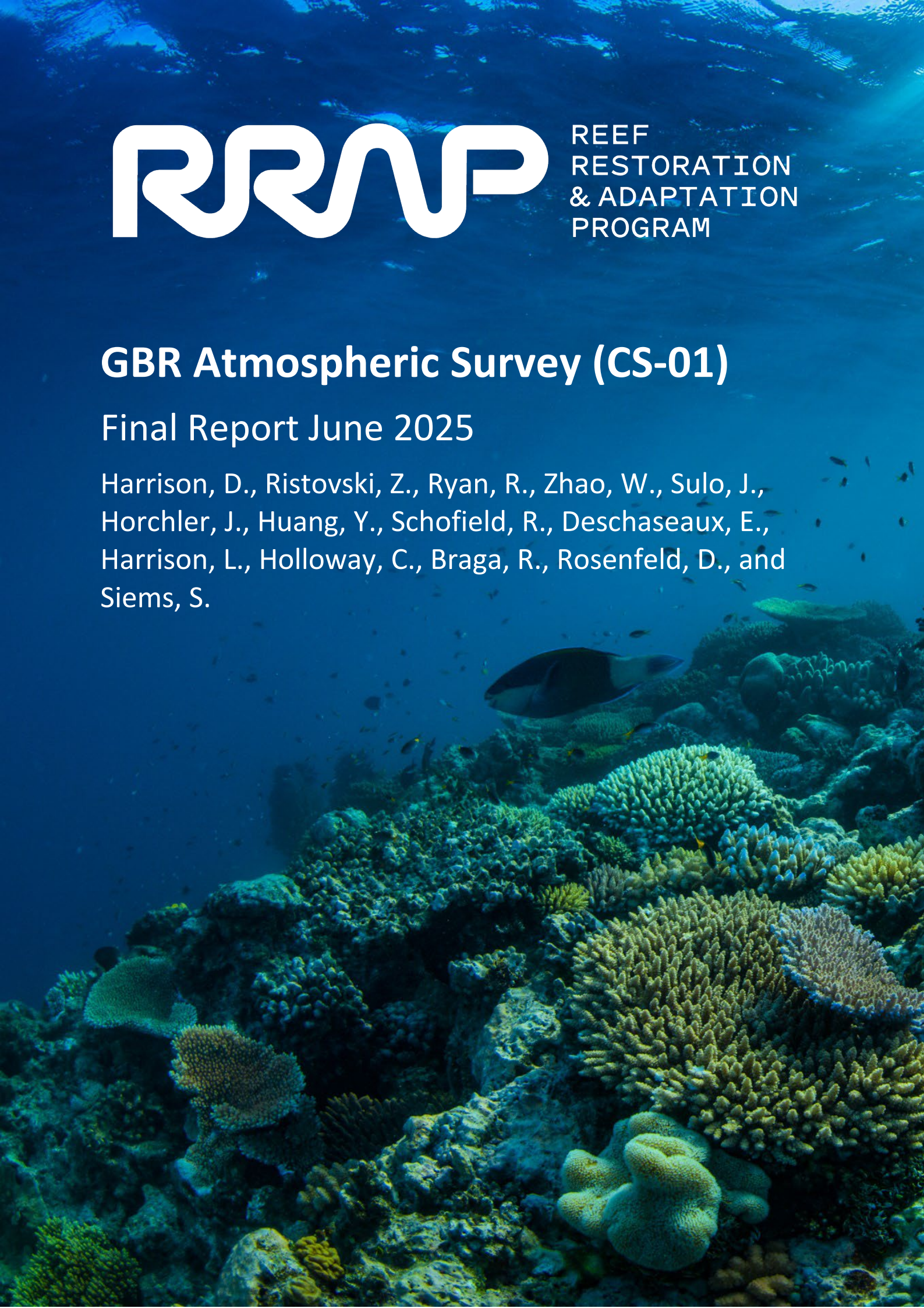


REEF  
RESTORATION  
& ADAPTATION  
PROGRAM

## **GBR Atmospheric Survey (CS-01)**

**Final Report June 2025**

Harrison, D., Ristovski, Z., Ryan, R., Zhao, W., Sulo, J.,  
Horchler, J., Huang, Y., Schofield, R., Deschaseaux, E.,  
Harrison, L., Holloway, C., Braga, R., Rosenfeld, D., and  
Siems, S.



## RRAP GBR Atmospheric Survey (CS-01) Final Report June 2025

Enquiries should be addressed to:

[Daniel.Harrison@scu.edu.au](mailto:Daniel.Harrison@scu.edu.au)

Cover Page: Coral Reef, Credit: Gary Cranitch, Queensland Museum

### This report should be cited as

Harrison, D., Ristovski, Z., Ryan, R., Zhao, W., Sulo, J., Horchler, J., Huang, Y., Schofield, R., Deschaseaux, E., Harrison, L., Holloway, C., Braga, R., Rosenfeld, D., and Siems, S. (2025) Reef Restoration and Adaptation Program – GBR Atmospheric Survey (CS-01) Final Report 2025. (33 pp).

### Copyright and Disclaimer

This report summarises work undertaken under *GBR Atmospheric Survey (CS-01)* in accordance with the Reef Restoration and Adaptation Program's *Cooling and Shading* Project Agreements. It provides a summarised, point-in-time synopsis of activities, methods, findings and outcomes completed in accordance with the approved project scope up to 30 June 2025.

All information reflects project scope and outcomes as of May-June 2025. Subsequent updates, analyses, or scientific developments are not included. This report should be read alongside any associated and publicly available technical reports, datasets, and publications for full detail. This report does not provide scientific inferences, policy guidance or operational instructions beyond the project's defined scope and duration.

This report is licensed under Creative Commons Attribution 4.0 Australia licence.

**Southern Cross University (SCU)** asserts the right to be recognised as author of the report in the following manner:

©Southern Cross University 2025 

Enquiries to use material including data contained in this report should be made in writing to **Southern Cross University**.

## Acknowledgement

This work was undertaken for the Reef Restoration and Adaptation Program (RRAP). Funded by the partnership between the Australian Governments Reef Trust and the Great Barrier Reef Foundation, partners include: the Australian Institute of Marine Science, CSIRO, the Great Barrier Reef Foundation, Southern Cross University, the University of Queensland, Queensland University of Technology and James Cook University.

The RRAP partners acknowledge Aboriginal and Torres Strait Islander Peoples as the first marine scientists and carers of Country. We acknowledge the Traditional Owners of the places where RRAP works, both on land and in sea Country. We pay our respects to Elders, past, present, and future, and their continuing culture, knowledge, beliefs, and spiritual connections to land and sea Country.

We specifically acknowledge and thank the following Traditional Owners of sea Country that this report relates to:

Location	Traditional Owner Group
Heron Island, One Tree Island and Gladstone	PCCC TUMRA, Gidarjil
Whitsundays	Ngaro
Broadhurst Reef and Davies Reef	Bindal and Manbarra

# Table of Contents

<b>1</b>	<b>Executive Summary</b>	<b>2</b>
<b>2</b>	<b>Background and Justification for the Research</b>	<b>3</b>
<b>3</b>	<b>Research Objectives and Key Findings</b>	<b>5</b>
<b>4</b>	<b>Future Research Recommendations</b>	<b>26</b>
<b>5</b>	<b>References</b>	<b>28</b>

## List of Figures

Figure 1: Summertime (Jan-Mar) Climatology (2016-2019). Produced using JAXA algorithms from Himawari-8 satellite data (Huang, in-prep).....	7
Figure 2: 23-year (1996-2018) summertime (Jan-Mar) cloud type climatology using the Cloud_CCI AVHRR-PM product (PM observations, 0.25° resolution; Huang, in-prep).....	8
Figure 3: The average measured number concentration of CCN particles vs. retrieved by satellite for eight days of overpass (30-01-2022, 31-01-2022, 01-02-2022, 04-02-2022, 17-02-2022, 18-02-2022, 19-02-2021, 21-02-2022, and 22-02-2022).....	11
Figure 4: Dependence of radiative effect over the Great Barrier Reef on cloud droplet number concentration ( $N_d$ ) for given cloud geometrical thickness (CGT) over four seasons. ....	13
Figure 5: The fraction of filtered liquid clouds for each grid from 2003 to 2020 for each season. ....	14
Figure 6: $NH_3$ mixing ratios in ppb obtained from NO3-CIMS, 10-min-cumulative rainfall in mm, and meteorological data (10-min averaged).....	17
Figure 7: Relation between MSA and SA in pre-rain cluster (a-c) as well as between HCl and HBr in the entire dataset used for clustering analysis (d-f). The data is coloured by wind speed (a, d). Subfigures (c) and (f) shows the relation for higher wind speed conditions while (b) and (e) for lower wind speed. ....	19
Figure 8: Cloud microphysical properties measured during Flight 20240221F1 at cloud bases of cumulus clouds.....	20
Figure 9: Sample analysis of hyperspectral scene showing (A) shortwave radiometric intensity ( $Wm^{-2}$ ) and resultant albedo (scale $\times 10000$ ) during the overpass, (B) processed albedo raster where brighter colours indicate higher albedo, (C) ratio of measured radiance.....	21
Figure 10: CCN number concentration, hygroscopicity parameter $\kappa$ , and CN number concentration for the marine periods MP (blue) and the continental periods CP (red) at 0.3 % SS. The black horizontal line in a box displays the median of the individual data. The lower and upper hinges represent the 25th and 75th percentiles. The upper and lower whiskers extend from the hinge to the largest or smallest measured values, respectively, but not more than 1.5 times the difference between the 25th and 75th percentiles. The mean is shown as grey points for the MP and grey triangles for the CP.....	22
Figure 11: Two-dimensional (2D) histograms of CCN and total particle number concentration and CCN and accumulation mode particle number concentration (a, b) and continental influence effect on CCN and total particle number concentration (c). The land fraction is calculated based on 72-hour HYSPLIT airmass back trajectories and presents the fraction of time the airmass was affected by continental or island emissions. .	23
Figure 12: High and low cloud visible at sunset over the Great Barrier Reef.....	27

## List of Tables

Table 1: Key findings of the Project aligned to the overarching and specific research questions for each sub-project. ....	5
Table 2: Dates of measurements with RV Magnetic position when the measurements took place near Davies Reef. Averaged CCN(S) spectra (Twomey equation ( $CCNS = N0 \cdot Sk$ )) for measurements between 7 am and 9 am local time. Similar to thermodynamic parameters: air temperature (T), dew point temperature (Td), and relative humidity (RH). The Lift Condensation Level (LCL), a proxy for cloud base height is also shown.....	10
Table 3: Summary of cloud properties over the GBR as retrieved from MODIS L2 cloud products (2003-2020), using the Tau-reflectance method of Rosenfeld et al. (2019).....	12
Table 4: Variation in the Project over time. ....	25

# 1 Executive Summary

The Cooling and Shading Research and Development (R&D) Sub-program (CS), under the Reef Restoration and Adaptation Program (RRAP), focuses on identifying methods to reduce coral bleaching stress by limiting solar radiation exposure over the Great Barrier Reef (GBR). This work includes the investigation of interventions such as Marine Cloud Brightening (MCB), misting, and fogging to either increase cloud reflectivity or create artificial shade. Given the GBR's scale—spanning over 2,000 kilometres—and the complexity of its meteorological environment, which includes trade winds, monsoonal systems, and tropical storms, a detailed understanding of atmospheric conditions is essential.

The GBR Atmospheric Survey Project (CS-01) was established to investigate key meteorological and aerosol processes that influence cloud formation and the potential for solar radiation management. The study places particular emphasis on aerosol-cloud interactions, turbulence in the marine boundary layer, and regional atmospheric variability, producing data critical to evaluating the feasibility of cooling interventions.

This Project combines satellite data, ground-based instruments, and airborne observations to assess atmospheric composition and behaviour across the region. Specific research efforts have focused on understanding cloud microphysics and aerosol characteristics, assessing the potential for MCB based on cloud condensation nuclei (CCN) distributions (or availability), and exploring how meteorological drivers such as heat fluxes and climate oscillations (including El Niño-Southern Oscillation (ENSO) and the Madden-Julian Oscillation (MJO)) influence bleaching risk. Observations from the field and satellite platforms have been used to validate and improve remote sensing methods and model outputs.

Initial findings indicate that natural aerosol concentrations exhibit significant spatial and temporal variability, affecting cloud reflectivity and broader meteorological parameters. These variations play a central role in shaping the GBR's cloud cover. The results also show that aerosol injections may have potential to brighten clouds, though further study is needed to understand their long-term effectiveness. The region's highly dynamic weather patterns and large-scale climate variability present ongoing challenges in reliably predicting the outcomes of shading interventions. Data limitations, especially a lack of high-resolution atmospheric observations including long term observations, underscore the importance of continued monitoring and expanded fieldwork.

The study has produced a valuable atmospheric dataset that enhances understanding of cloud behaviour over the GBR. This information supports the development of climate adaptation strategies and can inform policy aimed at reef protection. Moving forward, the research recommends further numerical modelling, expanded field deployments, and optimisation of aerosol delivery systems to refine and test Cooling and Shading techniques.

Overall, the GBR Atmospheric Survey Project (CS-01) provides a critical foundation for evaluating atmospheric interventions to protect the GBR. Sustained research efforts, improved modelling tools, and real-world testing are required to assess the full potential of these climate-based technologies in conserving coral reef ecosystems.

## 2 Background and Justification for the Research

The Cooling and Shading Sub-program is a central element of the Reef Restoration and Adaptation Program (RRAP), established to investigate the viability of engineering technologies that may help reduce coral bleaching. Techniques that aim to reduce solar radiation and thereby shade or cool corals on the Great Barrier Reef have been the focus of the first five years of the research and development program. Coral bleaching events, increasingly driven by marine heatwaves associated with climate change, represent a critical threat to coral reef ecosystems. To mitigate this risk, the RRAP Cooling and Shading Sub-program is examining potential interventions that can reduce thermal stress by either increasing cloud reflectivity or generating shading through the production of an artificial seawater fog. These interventions range in scale from site-specific applications at individual reefs to more ambitious regional efforts across large sections of the GBR Marine Park.

The GBR extends over 2,000 kilometres and spans a wide range of latitudes from the deep tropics through to the subtropics. The region's meteorology is shaped by a dynamic combination of trade winds, monsoon systems, tropical storms, and broader climate phenomena such as the El Niño-Southern Oscillation (ENSO) and the Madden-Julian Oscillation (MJO) (Richards et al. 2024). These drivers influence not only surface weather but also the formation, persistence, and radiative properties of marine boundary layer clouds, features that are particularly relevant to techniques like Marine Cloud Brightening (MCB). The thermodynamic structure of the atmosphere, along with variations in aerosol concentrations and turbulent mixing, further complicate predictions of how such interventions will perform under real-world conditions.

In response to this complexity, the GBR Atmospheric Survey Project (CS-01) (and the Atmospheric and Meteorological Monitoring Project (CS-02), which was combined into this project) was initiated to provide the scientific foundation required to evaluate and design Cooling and Shading interventions. A key driver of the work was the need to address the paucity of atmospheric measurements over the GBR by collecting a quality dataset with which various scales of atmospheric models could be developed, calibrated and validated. This project integrates satellite data, *in situ* measurements, and numerical modelling to characterise the key processes governing aerosol-cloud interactions, atmospheric chemistry, and regional meteorological variability in this region. A major focus of the research has been the role of cloud condensation nuclei (CCN), which are necessary for cloud droplet formation and strongly influence cloud microphysical properties and albedo. Understanding the natural distribution and variability of CCN across the GBR is essential for evaluating whether additional aerosols introduced by interventions such as MCB can effectively enhance cloud reflectivity. To support this, both ground-based and aircraft-deployed instrumentation have been used to measure aerosol concentration, composition and size distribution, cloud droplet characteristics, vertical wind structure, humidity, and radiative fluxes.

Satellite records have been analysed to build a climatology of cloud occurrence, thickness, and brightness across the region. This work includes the development of novel satellite retrieval techniques to estimate CCN concentrations remotely, which enables large-scale assessment of intervention potential and helps identify zones where cloud brightening may be most effective. These remote sensing products are complemented by extensive field campaigns that collect high-resolution observational data for validation and calibration. Aircraft-based sampling has been used to measure cloud microphysical properties and turbulence both within and above clouds, offering insights into the processes that govern aerosol dispersion, cloud formation, and radiative effects.

Another component of this Project's research has focused on the exchange of gases between the ocean and atmosphere, including biogenic volatile organic compounds (BVOCs) emitted by coral reef systems. These compounds can contribute to secondary aerosol formation and influence CCN availability, introducing a potential natural feedback mechanism between reef ecosystems and local cloud properties. Characterising the spatial and temporal variability of these emissions enhances understanding of the role the reef itself may play in shaping its atmospheric environment.

Finally, the project has examined how synoptic-scale meteorological conditions affect both coral bleaching risk and the feasibility of cooling interventions. By linking atmospheric datasets with ocean heat flux measurements and coral stress indicators, researchers are improving forecasts of when and where atmospheric interventions might be most beneficial. This integrated approach allows experimental findings to be contextualised within broader patterns of climate variability and used to inform adaptive management strategies.

The knowledge generated by this Project is directly informing the development of operational frameworks for proposed cooling technologies. The datasets generated are also already extensively in use for the development of atmospheric models of the Great Barrier Reef region (see the RRAP Environmental Modelling (CS-03) Final Project Report). By combining empirical observations with advanced numerical simulations, this research supports the design of targeted, evidence-based interventions that are responsive to environmental conditions and aligned with broader conservation objectives. In doing so, it contributes not only to immediate decision-making around intervention feasibility but also to the long-term goal of enhancing reef resilience under a changing climate.

### 3 Research Objectives and Key Findings

A current list of project outputs are listed on the RRAP website: [gbrrestoration.org](http://gbrrestoration.org). Key research objectives and findings are detailed below.

Table 1: Key findings of the Project aligned to the overarching and specific research questions for each sub-project.

Objective	Key Findings and/or Outcomes
<p>1. Capture a comprehensive process orientated snapshot of atmospheric interactions over the reef through collection and analysis of atmospheric data.</p>	<p>Field campaigns were conducted in December 2021 (RV Magnetic), February 2022, summer 2023, February 2024 and November - December 2024.</p> <ul style="list-style-type: none"> <li>• The December 2021 campaign was based near Townsville/Davies Reef/Magnetic Island and covered the mid-tropics with shipborne deployment of a suite of instrumentation to observe climate relevant baseline properties over the reef, including aerosol and greenhouse gas concentrations and meteorological parameters.</li> <li>• The 2022 February campaign was based over the vicinity of Townsville/Davies Reef/Magnetic Island, covering the mid-tropics with both ground-based and ship-based instrument deployments, aimed at continued coverage of the same climate relevant properties but timed at the end of the Austral summer, capturing intraseasonal variation in atmospheric conditions over the reef.</li> <li>• The February through to March 2023 campaign was based over the vicinity of Gladstone/Heron Island/One Tree Island, covering the subtropics with ground-based, ship-based and aircraft field observations. Detailed atmospheric composition was conducted at Heron Island.</li> <li>• The 2024 February campaign was based out of Hamilton Island, consisting of ground-based, ship-based and aircraft observations.</li> <li>• The December 2024 campaign was conducted at Heron Island and included ground-based observations using the same suite of instrumentation as in 2023, to assess year to year variability at a specific location.</li> </ul> <p>Within the scope of this Project, these campaigns made observations of the atmospheric composition, including various aerosols, clouds macro- and microphysics, atmospheric turbulence, atmospheric thermodynamics, and radiation. The campaigns captured representative snapshots of temporal and spatial variability in both mid- and sub-tropics, providing comprehensive measurements of CCN and aerosol number concentrations and meteorological variables, allowing for the characterisation of spatial and temporal variability of key baseline variables required for understanding the formation of clouds over the reef. The atmospheric chemistry spanned greenhouse gases, biogenic volatile organic compounds (BVOCs), sulphate and black carbon. The atmospheric chemistry measurements cover gas- and particle-phase measurements, allowing for characterisation of aerosol and CCN sources and particularly investigate the contribution of coral reefs to local CCN budget.</p>

Objective	Key Findings and/or Outcomes
	The meteorology was examined across a range of scales from global climate drivers, such as the ENSO index, to the synoptic meteorology.
2. Satellite derived cloud climatology of cloud macro, microphysical, life cycle (including diurnal) and precipitation characteristics over the reef during summer	<p>This main findings of this work are published in Zhao et al. (2022). A characterisation of cloud properties associated with precipitation in the region around the Great Barrier Reef (GBR) was constructed using decade-long (2007–2017) satellite observations from Moderate Resolution Imaging Spectroradiometer (MODIS) and Cloud-Aerosol Lidar and Infrared Pathfinder Satellite Observations (CALIPSO) combined with CloudSat. The spatial and vertical distributions of low-level cloud properties over the region were also investigated and discussed.</p> <p>The key findings indicated that high clouds are dominant over the low latitudes in summer and low-level clouds are dominant over the ocean and coast during the winter months at higher latitudes under a trade wind regime. A strong latitudinal dependence of total precipitation across the Greater GBR region is identified with a significant orographic enhancement near Cairns in the wet tropics. The largest land - ocean differences in warm cloud microphysical properties are found over the mid-latitudes strongly associated with orographic forcing, with these enhancements extending further east to the coral reef area. No significant differences in warm cloud properties between the actual GBR and the open ocean are identified.</p>

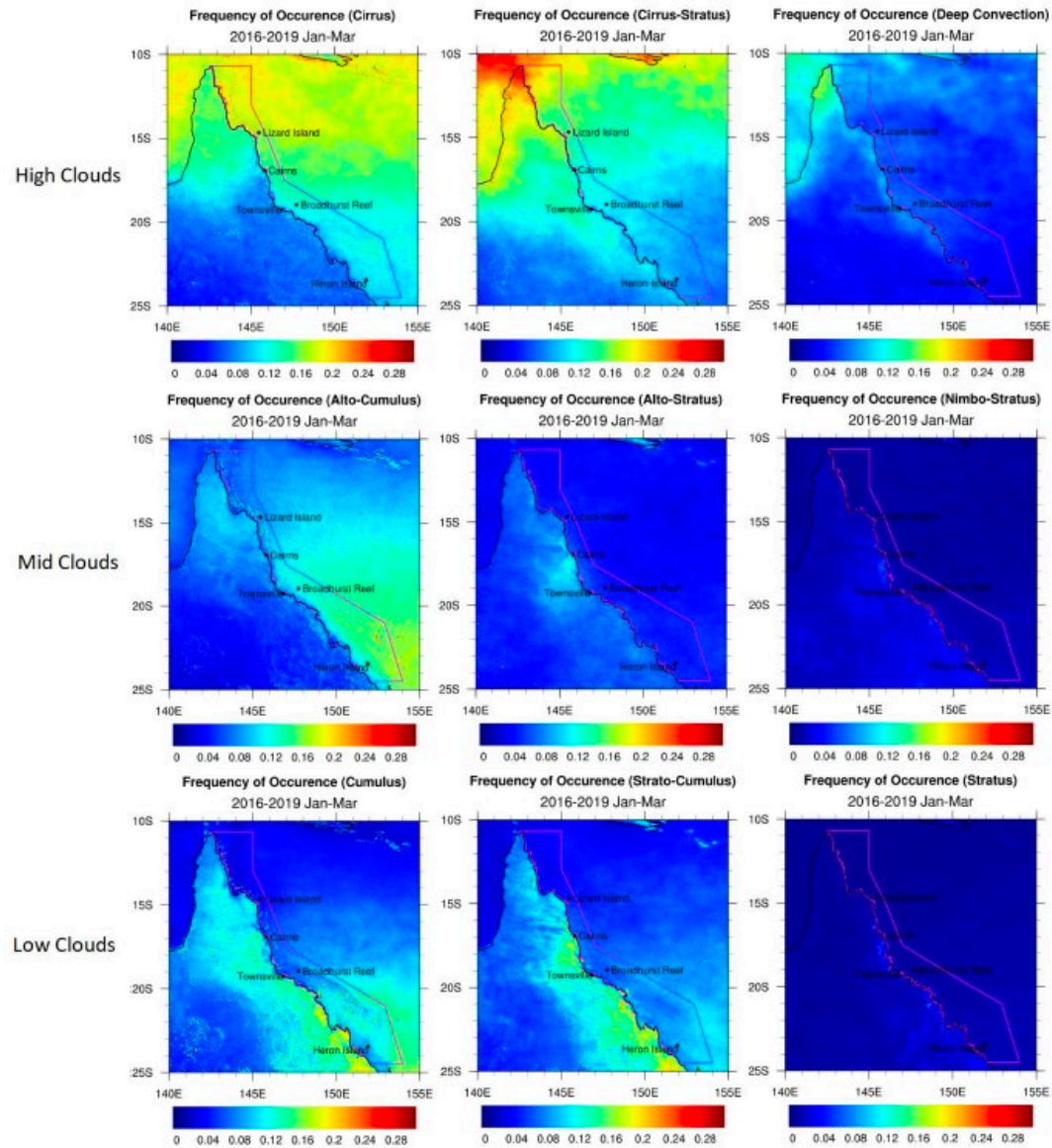
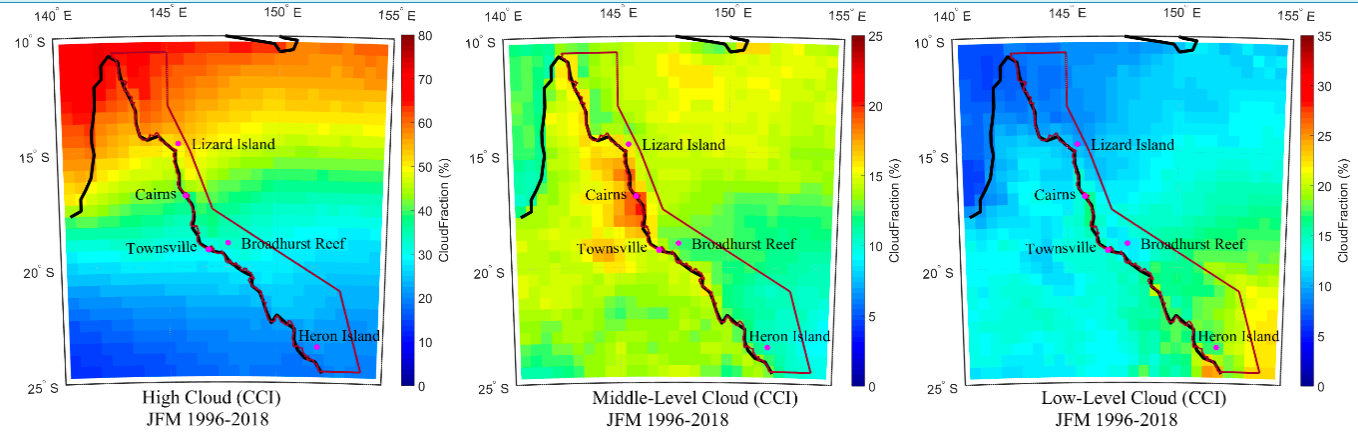


Figure 1: Summertime (Jan-Mar) Climatology (2016-2019). Produced using JAXA algorithms from Himawari-8 satellite data (Huang, in-prep).

**Objective**

**Key Findings and/or Outcomes**



*Figure 2: 23-year (1996-2018) summertime (Jan-Mar) cloud type climatology using the Cloud\_CCI AVHRR-PM product (PM observations, 0.25° resolution; Huang, in-prep)*

In general, different cloud types are observed over different regions and vary by season: high clouds are dominant over the low latitudes in summer, and low-level clouds are dominant over the ocean and coast during the winter months at higher latitudes under a trade wind regime. A strong latitudinal dependence of total precipitation across the Greater GBR region is identified with a significant orographic enhancement near Cairns in the wet tropics. MODIS and CloudSat-CALIPSO cloud observations show good agreement on significant differences in low-level cloud microphysical properties between the land and the ocean. The largest land–ocean differences in warm cloud microphysical properties are found over the mid-latitudes near 18°S, which is strongly associated with orographic forcing, with these enhancements extending further east to the coral reef area. However, the frequency of warm cloud is not enhanced upwind of the mountains in the wet tropics. In addition, no significant differences in warm cloud properties between the actual GBR and the open ocean are identified. These results suggest that low-level clouds over the GBR do not show any significant response to the reef-related microphysical perturbations.

Focussing on the 2021-2022 and 2022-2023 campaigns, the total cloud cover anomalies for both campaigns derived from MODIS observations suggest that reduced cloud fractions were evident during the main field campaign months (e.g. Jan-Feb 2022 and Mar 2023). This reduction in cloud cover was consistent with timing of the passage of the Madden-Julien Oscillation (MJO), a meteorological phenomenon that characterises heavy convection and precipitation across the tropics. Enhanced cloud cover was seen during the February 2023, which is largely contributed to the overpass of a severe tropical cyclone Gabrielle. Gabrielle was formed in the Coral Sea on 5th February and moving and developing into a tropical cyclone on 8th February when it passed the east of Willis Island. It was intensifying into a Category 3 tropical cyclone with the lowest central pressure of 958hPa and peak wind speed of 150 kilometres per hour (km/h). Gabrielle spent nearly 10 days off the Queensland coast, leading to a significant enhanced cloudiness across the domain.

Objective	Key Findings and/or Outcomes
<p>3. Analysis of aerosol – cloud condensation nuclei - cloud microphysical - albedo interactions under various thermodynamic conditions retrieved from satellite datasets over the reef to provide an early indication of the likely efficacy of cloud brightening</p>	<p>The effectiveness of added sea-spray aerosols for marine cloud brightening (MCB) depends strongly on the background concentrations of cloud condensation nuclei (CCN). This motivated the development of a novel satellite-based method to retrieve CCN concentrations as a function of water vapor supersaturation (<math>S_w</math>) over the Great Barrier Reef (GBR). The new methodology was validated successfully against ship-borne CCN measurements during the 2023 field campaign.</p> <p>Application of this methodology reveals background CCN concentrations ranging from <math>\sim 50 \text{ cm}^{-3}</math> at <math>S_w = 0.3\%</math> to <math>\sim 200 \text{ cm}^{-3}</math> at <math>S_w = 0.7\%</math>, with a mode of <math>\sim 100 \text{ cm}^{-3}</math> near <math>S_w = 0.4\%</math>. These concentrations are sufficiently low for a strong Twomey effect, making MCB potentially effective over much of the GBR. In contrast, air masses transported from land, especially from densely populated regions, carry much higher CCN concentrations, thereby diminishing the efficacy of MCB. The cloud-fraction (Albrecht) effect, however, tends to saturate at relatively low CCN concentrations (<math>\sim 60 - 100 \text{ cm}^{-3}</math>), indicating limited potential for additional negative radiative forcing through increased cloud cover.</p> <p>The observed CCN(<math>S_w</math>) spectra provide essential boundary layer conditions for regional cloud and MCB simulations, ensuring that background CCN levels are realistically represented. Since the radiative response of MCB is highly sensitive to the ambient CCN environment, accurate initialisation with measured CCN(<math>S_w</math>) spectra is critical to quantify the efficacy of cloud albedo modification.</p>
<p>4. Validation of satellite derived properties against in situ measurements. The retrieved cloud and CCN properties will be validated for the GBR region against field measured data throughout the duration of the project.</p>	<p>The number concentration of Cloud Condensation Nuclei (CCN) particles as a function of water vapor supersaturation (<math>S</math>), expressed as the activation spectra CCN(<math>S</math>), was evaluated over the Great Barrier Reef using in situ measurements and satellite retrievals. Data were collected during January–February 2022 in the vicinity of Broadhurst and Davies Reefs. The analysis focused on background conditions, considering CCN(<math>S</math>) measured for supersaturations in the range <math>0.1\% \leq S \leq 0.7\%</math>.</p> <p>CCN number concentrations were measured using a single-column Continuous-Flow Streamwise Thermal Gradient CCN Counter (CCNC-100, Droplet Measurement Technologies), following the method of Roberts and Nenes (2005). The instrument exposes sampled aerosol particles to a controlled supersaturation, allowing particles to grow by water uptake according to their size and chemical composition. Particles that activate and grow to diameters larger than <math>1 \mu\text{m}</math> are counted as CCN at the corresponding <math>S</math>. Calibration was performed according to Rose et al. (2008), ensuring measurement accuracy. The instrument operated at a temporal resolution of 1 Hz.</p> <p>Table 2 summarises the RV Magnetic position, thermodynamic measurements, and CCN(<math>S</math>) spectra collected during on-site sampling over Davies Reef. The CCN(<math>S</math>) spectra were fitted using a power-law parameterisation of the form:</p> $CCN(S) = C \cdot S^k \quad (1)$ <p>where <math>C</math> is the scaling factor and <math>k</math> is the activation exponent. Higher <math>k</math> values indicate a stronger sensitivity of CCN activation to supersaturation, typically associated with aerosol-rich regimes, while lower <math>k</math> values correspond to CCN-limited conditions (Twomey, 1959).</p>

*Table 2: Dates of measurements with RV Magnetic position when the measurements took place near Davies Reef. Averaged CCN(S) spectra (Twomey equation ( $CCN(S) = N_0 \cdot S^k$ )) for measurements between 7 am and 9 am local time. Similar to thermodynamic parameters: air temperature (T), dew point temperature (Td), and relative humidity (RH). The Lift Condensation Level (LCL), a proxy for cloud base height is also shown.*

Date	Vessel Position (lon; lat)	CCN spectra	P (hPa)	T (°C)	Td (°C)	RH (%)	LCL (m)
30/1/2022	147.72; -18.87	CCN = 330.8 * S ^ (0,52)	1006.5	28.1	20.8	64.7	909.6
31/1/2022	147.55; -18.84	CCN = 174.6 * S ^ (0,45)	1005.9	28.1	22.3	70.8	724.0
1/2/2022	147.76; -19.13	CCN = 300.7 * S ^ (0,32)	1005.6	28.5	22.9	71.8	698.6
2/2/2022	147.42; -18.90	CCN = 228 * S ^ (0,36)	1004.3	28.6	22.7	70.6	732.5
3/2/2022	147.50; -18.92	CCN = 287.2 * S ^ (0,57)	1001.3	28.7	24.2	76.8	559.8
4/2/2022	147.68; -18.86	CCN = 124.9 * S ^ (0,63)	999.5	26.9	23.3	80.9	444.7
16/2/2022	147.02; -18.49	CCN = 150,2 * S ^ (0,33)	1009.2	27.4	22.9	76.6	560.6
17/2/2022	147.72; -18.86	CCN = 107.2 * S ^ (0,33)	1008.2	27.3	23.2	78.3	513.4
18/2/2022	147.72; -18.86	CCN = 144.8 * S ^ (0,38)	1007.8	27.9	22.8	73.8	638.5
19/2/2022	147.72; -18.86	CCN = 285.6 * S ^ (0,41)	1008.6	27.9	22.3	71.7	699.2
20/2/2022	147.62; -18.82	CCN = 206.3 * S ^ (0,68)	1006.6	27.3	21.8	72.1	683.9
21/2/2022	147.69; -18.88	CCN = 262.6 * S ^ (0,43)	1006.3	27.8	22.5	73.3	653.1
22/2/2022	147.69; -18.88	CCN = 223.4 * S ^ (0,48)	1007.1	27.9	22.4	72.0	689.3

Satellite-based CCN(S) retrievals for marine clouds were obtained using the methodology proposed by Rosenfeld et al. (2016). These estimates were derived from imagery captured by the Visible Infrared Imaging Radiometer Suite (VIIRS) aboard the Suomi NPP satellite (Hillger et al. 2013; Hillger et al. 2014). The CCN(S) spectra retrieved from satellite observations were compared with in situ measurements collected onboard the RV Magnetic.

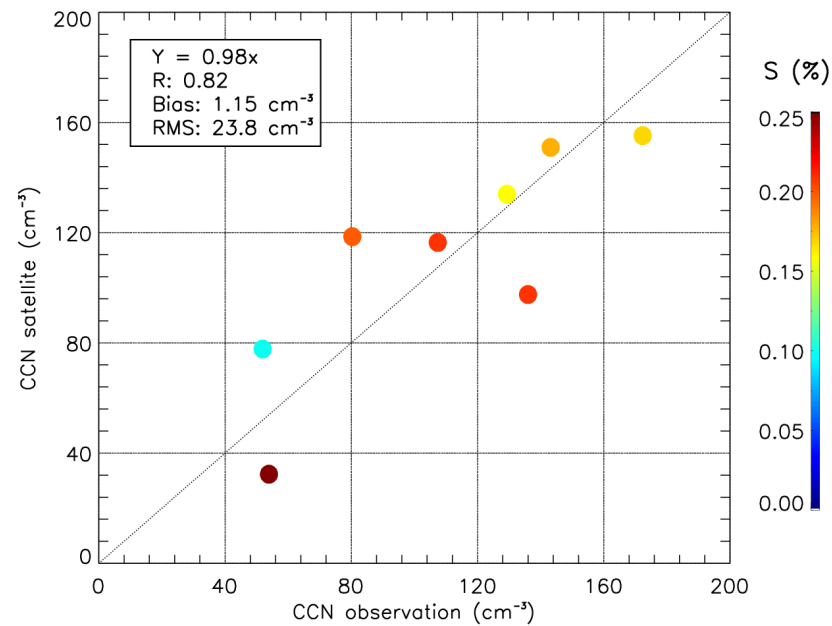


Figure 3: The average measured number concentration of CCN particles vs. retrieved by satellite for eight days of overpass (30-01-2022, 31-01-2022, 01-02-2022, 04-02-2022, 17-02-2022, 18-02-2022, 19-02-2021, 21-02-2022, and 22-02-2022).

Figure 3 shows the comparison between measured and satellite-retrieved CCN concentrations over Davies Reef. The results demonstrate a strong correlation, indicating that satellite-derived CCN(S) retrievals are consistent with high-resolution in situ measurements. This agreement validates the applicability of satellite-based methodologies for characterising CCN activation spectra in remote marine environments.

A detailed evaluation of the measured CCN(S) spectra in comparison with satellite-derived retrievals over the GBR has been developed as an internal report and is being prepared for publication Braga et al. (*in-prep*).

Climatology of satellite-retrieved low cloud properties and their susceptibility to cloud drop concentrations was done for the GBR region based on MODIS data between 2003 and 2020. It was found that the occurrence of low layer clouds that would be potentially susceptible to seeding effects during summer is 20% at the north and increases to 55% at the south. Most of the seeding effect on reflected solar radiation is expected from the albedo effect. A significant cloud cover effect is expected only when drop concentrations is smaller than  $\sim 30 \text{ cm}^{-3}$ . These conditions occur in  $\sim 40\%$  of the low clouds. The south part of the GBR has the most frequent seeding opportunities with suitable clouds.

Objective	Key Findings and/or Outcomes						
	<p><i>Table 3: Summary of cloud properties over the GBR as retrieved from MODIS L2 cloud products (2003-2020), using the Tau-reflectance method of Rosenfeld et al. (2019).</i></p>						
	N <sub>d</sub> [cm <sup>-3</sup> ]	% (N <sub>d</sub> <30)	CF(mask)	CF(tau)	CGT [m]	Re [μm]	CRE [Wm <sup>-2</sup> ]
Annual	53	30	0.44	0.32	386	18.9	-83
North	54	30	0.42	0.29	390	19.2	-77
Center	54	30	0.42	0.29	390	19.2	-77
South	60	30	0.40	0.28	403	19.1	-74
DJF							
North	41	47	0.32	0.21	390	19.9	-56
Center	41	47	0.34	0.23	379	19.8	-61
South	48	38	0.37	0.26	380	19.1	-71
JJA							
North	62	23	0.52	0.40	409	18.3	-105
Center	68	30	0.50	0.36	423	18.6	-98
South	78	30	0.45	0.32	434	18.8	-84

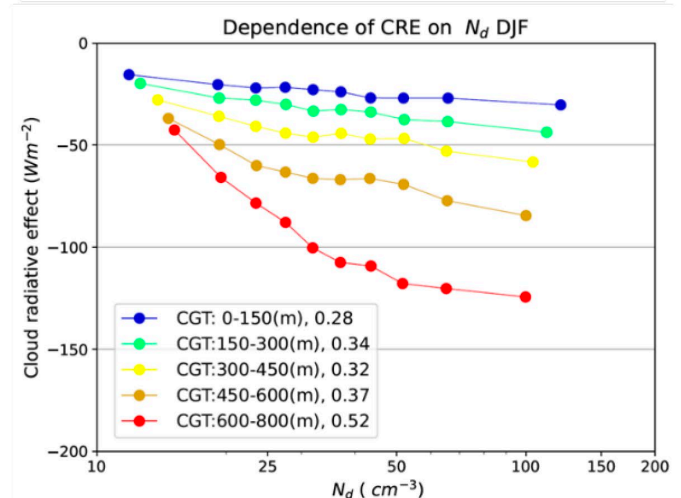
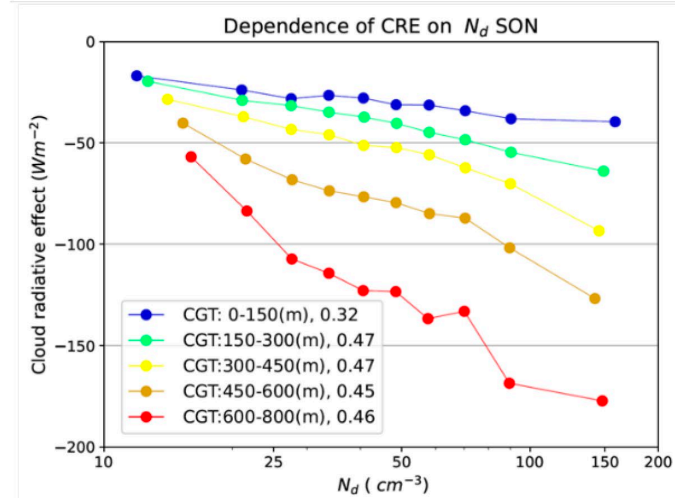
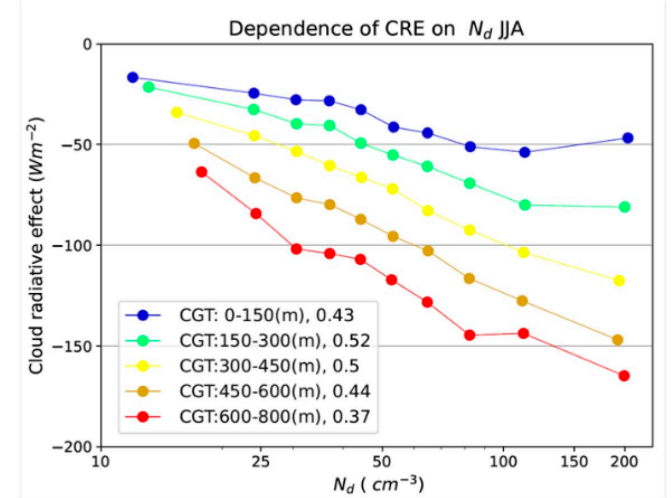
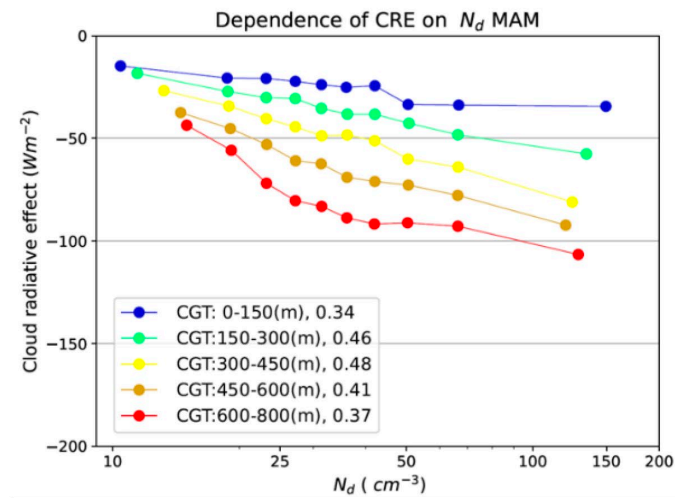


Figure 4: Dependence of radiative effect over the Great Barrier Reef on cloud droplet number concentration ( $N_d$ ) for given cloud geometrical thickness (CGT) over four seasons.

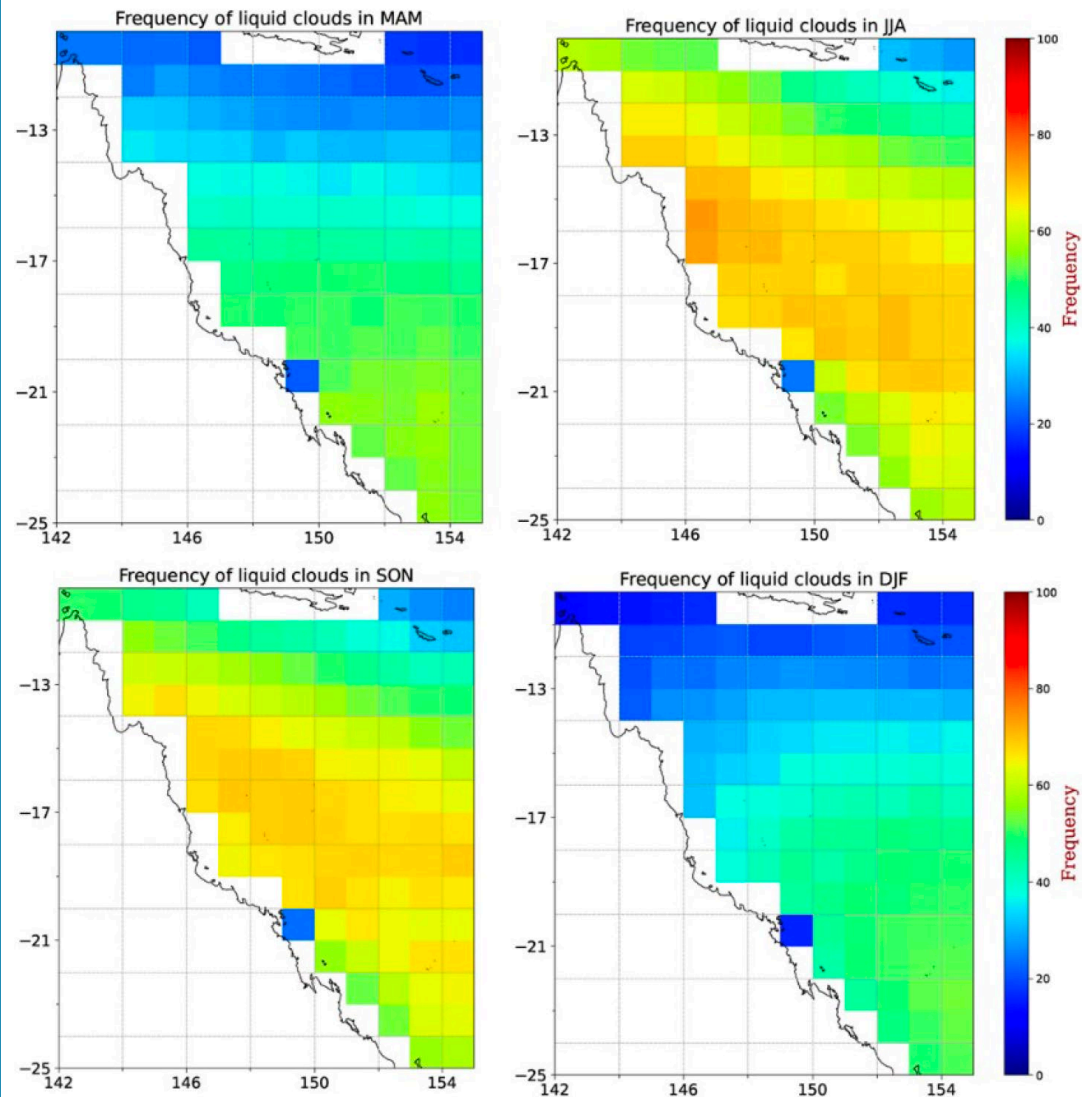


Figure 5: The fraction of filtered liquid clouds for each grid from 2003 to 2020 for each season.

Objective	Key Findings and/or Outcomes
<p>5. Surface-based measurements to derive cloud, aerosol, and precipitation properties including, miniMPL, MAX-DOAS, three 24 GHz Micro Rain Radars (MRR-2s) paired with Parsivel disdrometers. Complementing standard weather station observations and providing continuous 3D data fields of aerosol, cloud, and precipitation properties.</p>	<p>A combination of collocated Himawari-8/9 observations and ground-base in-situ observations (i.e. Micro Rain Radar (MRR) and disdrometer) allowed us to explore the presence of precipitation that is associated with warm cloud and the corresponding cloud and precipitation properties across the campaign sites. The analyses of warm cloud properties at offshore and onshore campaign sites for 2021/2022 summer campaign, distinguishing between precipitating and non-precipitating clouds. Precipitating clouds generally exhibited higher, cooler cloud tops with larger droplets at both sites. Onshore clouds tend to rise higher with cooler tops regardless of precipitation, likely due to coastal or orographic effects. It was interesting to note that warm clouds with larger optical depth were mostly observed at offshore site, though the droplets were detected with smaller effective radius. It is considered that this might be a result of abundant water vapour over the water compared to land, leading to a higher droplet number concentration.</p> <p>Vertical profiles of aerosol extinction were retrieved from Multi-Axis Differential Optical Absorption Spectrometer (MAX-DOAS) and Mini Micro Pulse Lidar (MPL) observations throughout the campaign. These were collated into diurnal average profiles. Afternoon enhancements in normalised relative backscatter in the free troposphere were seen to grow in altitude from around six to eight kilometres (km) as the afternoon progresses, which may have been due to the afternoon convective development of free tropospheric clouds. Aerosol extinction was more variable in the daytime (mean <math>0.018 \pm 0.035 \text{ km}^{-1}</math> between 8 am and 6 pm) than at night (mean <math>0.011 \pm 0.015 \text{ km}^{-1}</math> otherwise). Mean daytime aerosol extinction vertical profiles revealed that aerosol layers with extinction <math>&gt; 0.05 \text{ km}^{-1}</math> often extended beyond 2 km altitude. Given that the MPL and drone observations showed that the Planetary Boundary Layer Height (PBLH) was not extending beyond 1.5 km altitude, the aerosol layers detected up to 2 km extended beyond the boundary layer and may be associated with evaporation from clouds (Ryan et al. 2025).</p>
<p>6. Characterise climate and atmospheric relevant gases, air-sea gas exchange, black carbon, and scattering properties. The approach includes using Equilibrium Inlet – Proton-transfer-reaction mass spectrometry and separate temperature-controlled aerosol inlet with manifold enabling simultaneous observation of black carbon (MAAP), scattering properties (polar Nephelometer), H<sub>2</sub>SO<sub>4</sub>, dimethylsulfide and DMSO (Chemical Ionisation Mass Spectrometer (CIMS)), greenhouse gases (CO<sub>2</sub>, CO, CH<sub>4</sub>, N<sub>2</sub>O, etc.)</p>	<p>Biogenic volatile organic compounds (BVOCs) are gases that are emitted by both terrestrial and marine environments and that play key roles in the Earth’s radiation budget and in various biological processes at the cellular level. The BVOC team of the RRAP Cooling and Shading Sub-program conducted 1) two major field campaigns along the central and southern GBR in the summer of 2021-2022 and 2023, respectively, to estimate coral-reef derived BVOC emissions under natural environmental conditions during the hot summer months and 2) investigated the coral BVOC response to thermal-stress on adult (Heron Island, February 2023) and recruit (Townsville, February 2024) Acropora corals of the GBR in semi-static chamber experiments, both using a state-of-the-art proton-transfer-reaction mass spectrometer (PTR-MS).</p> <p>Through the first comprehensive baseline survey for the Cooling and Shading Sub-program of RRAP, dissolved and atmospheric concentrations of climatically-relevant BVOCs (dimethyl sulfide (DMS), methanethiol (MeSH), isoprene and monoterpenes) in the central GBR were quantified semi-continuously. This data was used to estimate high-resolution emission fluxes and determine the baseline BVOC signature of coral reef waters in the austral summer. Results indicated that the central GBR is a net source of climatically relevant BVOCs in summer (Deschaseaux et al. 2025). Interestingly, a coastward gradient was observed for dissolved concentrations and emission fluxes of BVOCs, which was expected for isoprene and monoterpene (originating dominantly from terrestrial sources) but not for DMS and MeSH (marine sourced BVOCs). The increase in dissolved BVOC concentrations with proximity to the coast were attributed to a coastward gradient for chlorophyll-a (chl-a) and nutrient concentrations. Once fed into existing models, these BVOC concentrations and fluxes can aid with</p>

Objective	Key Findings and/or Outcomes
	<p>predictions on the fate of BVOC emissions under future climate change scenarios and on the potential feedback effect of future BVOC emissions on the local climate of the GBR. Preliminary results from coral chamber experiments indicate an upregulation of DMS and MeSH as a response to heat stress, with interestingly a greater response when shade was applied alongside heat to mimic the shading regime being developed by the RRAP Cooling and Shading Sub-program.</p> <p>Ammonia (NH<sub>3</sub>) is a key atmospheric gas influencing secondary inorganic aerosol formation, new particle formation, and CCN activity, particularly in marine environments. We investigated NH<sub>3</sub> emissions on Heron Island, during the 2023 measurements campaign, using active, passive, and nitrate-chemical ionisation mass spectrometer (NO<sub>3</sub>-CIMS) (real time) sampling methods. NH<sub>3</sub> concentrations varied almost two orders of magnitude, ranging from seven to 483 parts per billion (ppb), with average values of 39 ± 19 ppb (passive sampling), and 62 ± 26 ppb (NO<sub>3</sub>-CIMS). All three methods showed consistent NH<sub>3</sub> trends, with a strong correlation between active and NO<sub>3</sub>-CIMS data, confirming the reliability of the latter technique. Precipitation was the primary driver of NH<sub>3</sub> fluctuations, with concentrations increasing significantly within 30 minutes to a few hours after rainfall events (Fig 7). Laboratory experiments using bird guano further demonstrated that precipitation, rather than temperature, was the dominant factor controlling NH<sub>3</sub> emissions. These findings highlight NH<sub>3</sub>'s dynamic behaviour and its sensitivity to environmental conditions. Given NH<sub>3</sub>'s role in aerosol formation, its variability has important implications for atmospheric chemistry and climate. This provided valuable insights into NH<sub>3</sub> emissions in fragile marine ecosystems like the GBR, emphasising the need for further research on its broader environmental impacts.</p>

Objective

Key Findings and/or Outcomes

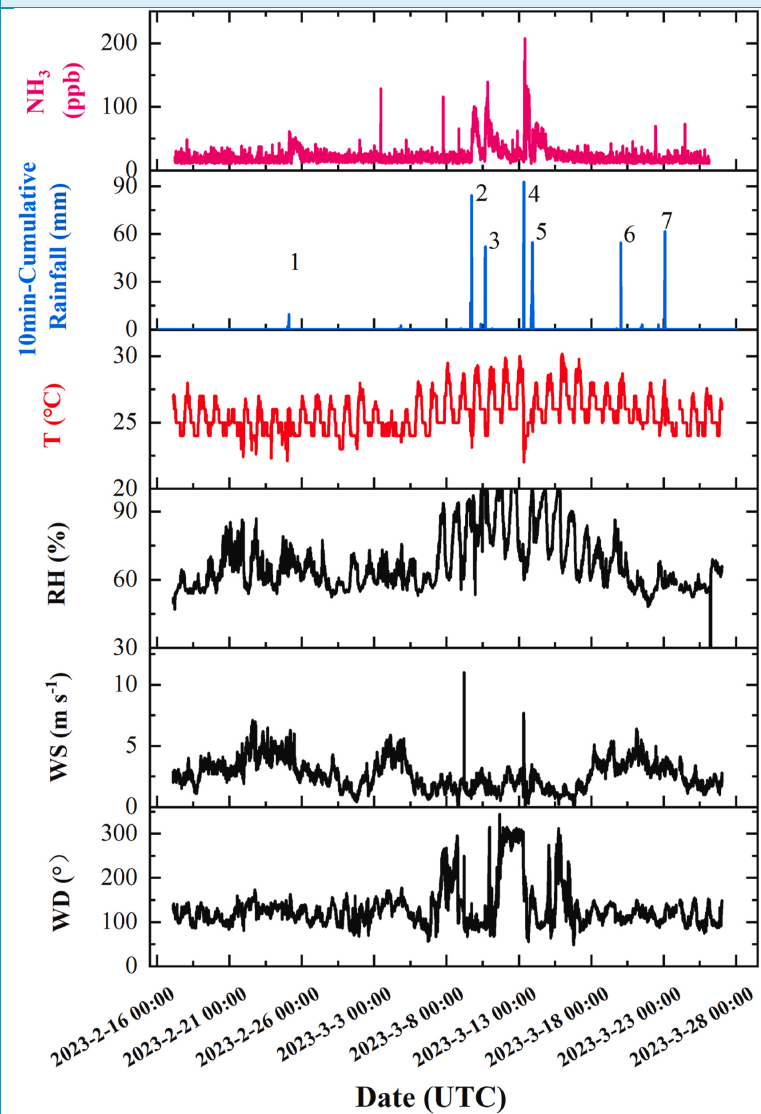
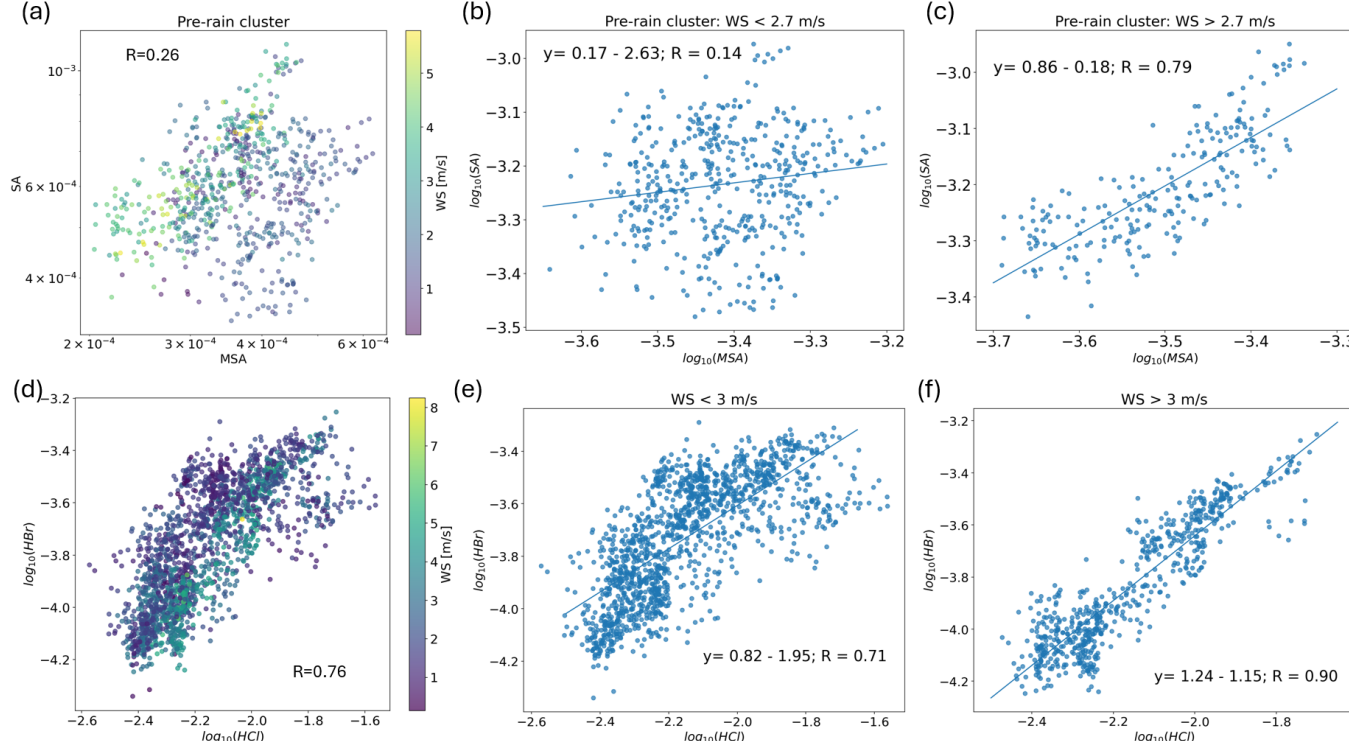
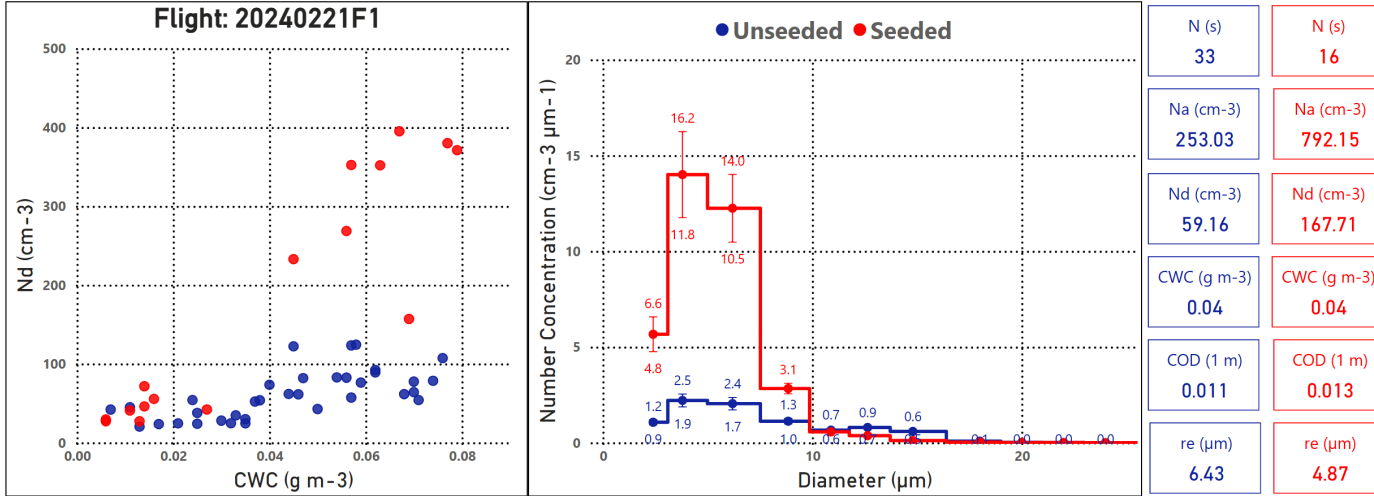


Figure 6:  $\text{NH}_3$  mixing ratios in ppb obtained from  $\text{NO}_3$ -CIMS, 10-min-cumulative rainfall in mm, and meteorological data (10-min averaged).

Objective	Key Findings and/or Outcomes
	<p>The isotopic variability of ammonia (<math>\delta^{15}\text{N-NH}_3</math>) values further confirm that <math>\text{NH}_3</math> volatilisation from seabird guano after precipitation is the primary source of atmospheric <math>\text{NH}_3</math> on the island. Increased moisture promotes microbial decomposition of uric acid, driving elevated <math>\text{NH}_3</math> emissions and influencing the observed isotopic composition (Wu et al. 2025). These findings have been published in the journal Atmospheric Environment.</p> <p>Alongside <math>\text{NH}_3</math> and amines, in marine environments, sulfuric acid (<math>\text{H}_2\text{SO}_4</math>), methane sulfonic acid (<math>\text{CH}_3\text{SO}_3\text{H}</math>), and halogenated acids such as perchloric acid (<math>\text{HClO}_4</math>) and iodic acid (<math>\text{HIO}_3</math>), along with hydrogen halides (<math>\text{HI}</math>, <math>\text{HCl}</math>, <math>\text{HF}</math>), play key roles in nucleation processes alongside <math>\text{NH}_3</math> and amines. Observations from Heron Island show that elevated <math>\text{NH}_3</math> levels coincide with increased concentrations of <math>\text{H}_2\text{SO}_4</math>, <math>\text{CH}_3\text{SO}_3\text{H}</math>, and <math>\text{HF}</math>. However, despite these elevated concentrations, no corresponding increase in particle number concentrations or ammonium and organic aerosol levels was observed, indicating that high <math>\text{NH}_3</math> and acid concentrations alone do not necessarily drive new particle formation.</p> <p>Our studies provided the first direct quantification of aerosol chemical composition and associated gas-phase compounds over the Great Barrier Reef (GBR) during summer, based on observations at Heron Island. Submicron non-refractory aerosol mass was dominated by sulphate (63%) and organics (30%), reflecting contributions from marine dimethyl sulfide (DMS) oxidation and local biological activity. Gas-phase measurements included sulfuric acid (<math>\text{H}_2\text{SO}_4</math>), methanesulfonic acid (MSA), halogen species (<math>\text{HCl}</math>, <math>\text{HBr}</math>, <math>\text{HI}</math>), and ammonia (<math>\text{NH}_3</math>), revealing strong correlations between MSA and <math>\text{H}_2\text{SO}_4</math> and between <math>\text{HCl}</math> and <math>\text{HBr}</math> under high wind speeds (Fig. 8.). Rain events triggered sharp increases in <math>\text{NH}_3</math> concentrations, linked to volatilisation from seabird guano, while diethylamine (DEA) peaked during clean post-rain periods under low coagulation sinks. Clustering analysis identified pre-rain, rain, post-rain, unstable, clean, and high-organics regimes, each with distinct aerosol and gas-phase signatures. Overall, the results show that while aerosol composition remains relatively stable, gas-phase precursors and meteorological conditions—particularly precipitation and wind speed—play a critical role in shaping aerosol dynamics. These findings provide a summer-specific characterisation of GBR atmosphere, relevant for assessing reef Cooling and Shading strategies under the Reef Restoration and Adaptation Program (Okuljar et al. 2025, manuscript submitted for publication).</p>

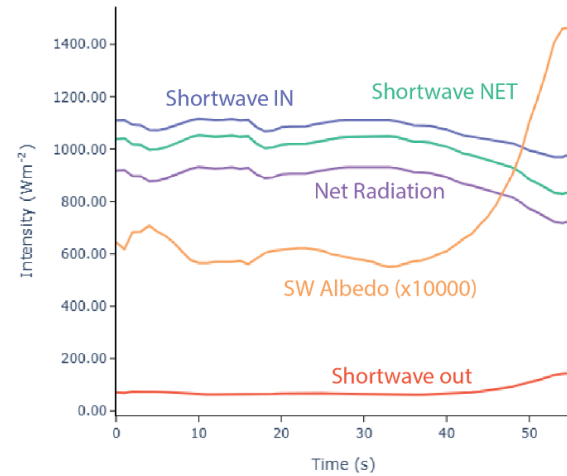
Objective	Key Findings and/or Outcomes
	 <p data-bbox="649 1037 1993 1125"><i>Figure 7: Relation between MSA and SA in pre-rain cluster (a-c) as well as between HCl and HBr in the entire dataset used for clustering analysis (d-f). The data is coloured by wind speed (a, d). Subfigures (c) and (f) shows the relation for higher wind speed conditions while (b) and (e) for lower wind speed.</i></p>
7.	<p data-bbox="197 1157 593 1316">Within cloud microphysical measurements of cloud droplet size distributions, interstitial aerosols, liquid water content, 3D winds, and turbulence.</p> <p data-bbox="649 1157 2016 1444">The research aircraft was available for the 2023 and 2024 field campaigns. During the MCB campaign the cloud microphysical properties were measured using a Cloud Combination Probe (CCP). CCP combines two detectors, the Cloud Droplet Probe (CDP) and the grayscale Cloud Imaging Probe (CIPGs), which allow the measurement of droplets with size range of 3 - 960 micrometre (<math>\mu\text{m}</math>). During the 2023-2024 field campaigns the resulting uncertainty in the droplet concentration (Nd) and cloud droplet effective radius (<math>r_e</math>) by CCP-CDP was about 10-15%. A hot-wire instrument that measure liquid water content was used as a reference for comparison with the integrated water content (CWC) from the droplet size distribution of CCP-CDP probe. Since the CWC was derived from a smaller set of physical parameters we observed an overall maximum uncertainty of <math>\sim 30\%</math>, (typical values observed for this type of probe). Figure 8 illustrates the cloud properties measured for seeded and unseeded (background) clouds during Flight 20240221F1. The seeding procedure produced a clear Twomey effect on the</p>

Objective	Key Findings and/or Outcomes																								
	<p>microphysical properties of clouds (average values of cloud properties and aerosol concentrations (Na) are shown on the right). The average Nd increased from 59.2 to 167.7 cm<sup>-3</sup> and re decreased from 6.43 to 4.87 μm, for similar range of CWC measurements. The estimated cloud optical depth (COD) of seeded clouds showed an increase of ~ 15% on average and about 50% for cloud passes with CWC &gt; 0.04 g m<sup>-3</sup>.</p> <div data-bbox="669 408 2038 906" style="border: 1px solid black; padding: 10px;">  <table border="1" data-bbox="1809 411 2033 903"> <tbody> <tr> <td>N (s)</td> <td>N (s)</td> </tr> <tr> <td>33</td> <td>16</td> </tr> <tr> <td>Na (cm<sup>-3</sup>)</td> <td>Na (cm<sup>-3</sup>)</td> </tr> <tr> <td>253.03</td> <td>792.15</td> </tr> <tr> <td>Nd (cm<sup>-3</sup>)</td> <td>Nd (cm<sup>-3</sup>)</td> </tr> <tr> <td>59.16</td> <td>167.71</td> </tr> <tr> <td>CWC (g m<sup>-3</sup>)</td> <td>CWC (g m<sup>-3</sup>)</td> </tr> <tr> <td>0.04</td> <td>0.04</td> </tr> <tr> <td>COD (1 m)</td> <td>COD (1 m)</td> </tr> <tr> <td>0.011</td> <td>0.013</td> </tr> <tr> <td>re (μm)</td> <td>re (μm)</td> </tr> <tr> <td>6.43</td> <td>4.87</td> </tr> </tbody> </table> </div> <p><i>Figure 8: Cloud microphysical properties measured during Flight 20240221F1 at cloud bases of cumulus clouds.</i></p>	N (s)	N (s)	33	16	Na (cm <sup>-3</sup> )	Na (cm <sup>-3</sup> )	253.03	792.15	Nd (cm <sup>-3</sup> )	Nd (cm <sup>-3</sup> )	59.16	167.71	CWC (g m <sup>-3</sup> )	CWC (g m <sup>-3</sup> )	0.04	0.04	COD (1 m)	COD (1 m)	0.011	0.013	re (μm)	re (μm)	6.43	4.87
N (s)	N (s)																								
33	16																								
Na (cm <sup>-3</sup> )	Na (cm <sup>-3</sup> )																								
253.03	792.15																								
Nd (cm <sup>-3</sup> )	Nd (cm <sup>-3</sup> )																								
59.16	167.71																								
CWC (g m <sup>-3</sup> )	CWC (g m <sup>-3</sup> )																								
0.04	0.04																								
COD (1 m)	COD (1 m)																								
0.011	0.013																								
re (μm)	re (μm)																								
6.43	4.87																								
<p>8. Above and below cloud measurement of upwelling and downwelling radiation respectively from over and underwing radiometers on the aircraft to determine cloud albedo and relate it to cloud microphysical properties during the field study.</p>	<p>The radiometer onboard the aircraft measures upwelling and downwelling radiation which can be used to calculate albedo. However, this instrument integrates the radiation over the entire up and down looking hemispheres and is therefore not sensitive to patchy clouds. The hyperspectral camera measures spatially and spectrally resolved radiation measurements. Conversion of measured quantities into transferable units involves substantial post-processing of data and the modelling of the radiative transfer of sunlight through the atmosphere and reflection from surfaces in the image. After this processing we obtain an image of reflectance for each pixel and spectral band from which the albedo can be calculated. Seeded clouds should appear to have a higher albedo than unseeded clouds.</p> <p>Other cloud properties can also be derived from specific wavelengths in the measured image. Oxygen in the atmosphere weakly absorbs light near 760 nm, given the amount of oxygen in the atmosphere is known and well mixed, the depth of this absorption is governed by the path length that light takes to the observer. Radiative transfer modelling of this absorption band has allowed us to determine the pixel resolved cloud top heights from the hyperspectral images. Similar methods can be used to determine effective radius and number concentration of cloud droplets changes in these also would indicate cloud seeding; this work is ongoing.</p>																								

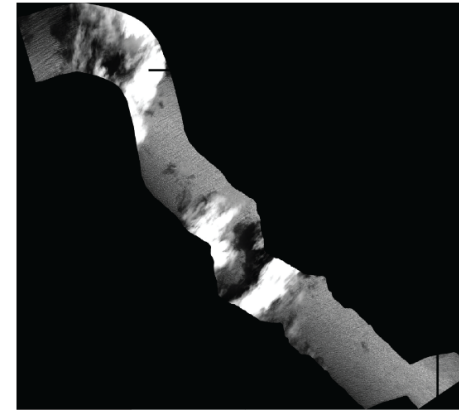
Objective

Key Findings and/or Outcomes

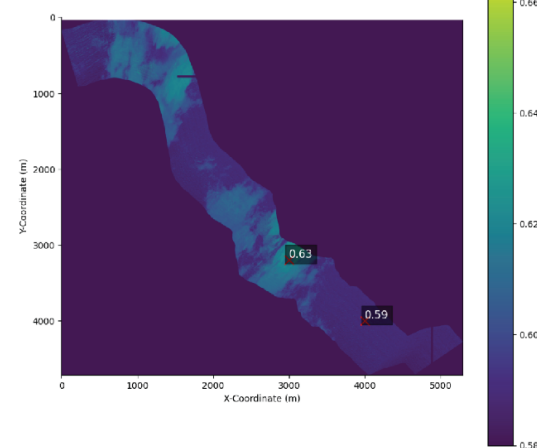
Radiometer results during cloud over pass



Albedo map of cloud from Hyperspectral image



Oxygen absorption depth ratio



Calculated Surface Heights

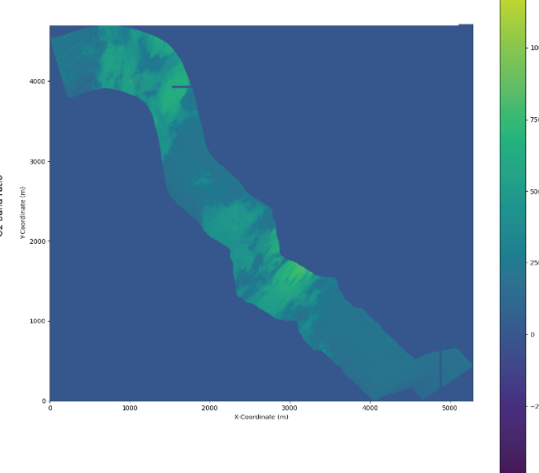
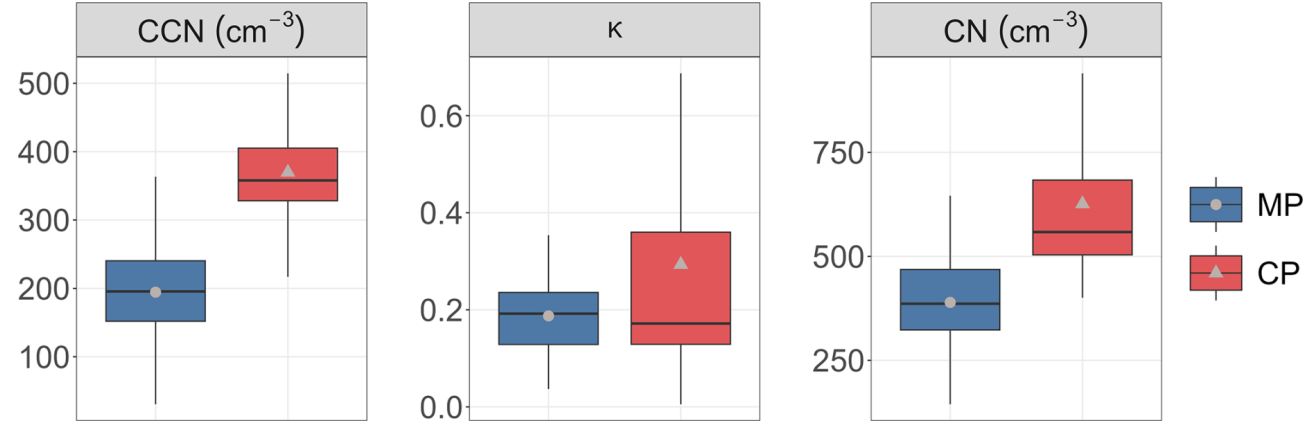


Figure 9: Sample analysis of hyperspectral scene showing (A) shortwave radiometric intensity (Wm<sup>-2</sup>) and resultant albedo (scale x10000) during the overpass, (B) processed albedo raster where brighter colours indicate higher albedo, (C) ratio of measured radiance.

Objective	Key Findings and/or Outcomes
<p>9. Aerosol size distribution, concentration, composition, optical, and hygroscopic properties from continuous surface-based measurement within the marine boundary layer and vertical profiles from the manned/unmanned airborne platforms during the field study.</p>	<p>An analysis of the ship observations finds that the GBR typically experiences low aerosol and CCN concentrations, with air masses arriving at the reef being typically clean marine air masses. A minority of the air masses measured contained notable reef or land influences, suggesting that properties of transported clean marine air dominate the aerosol properties over the reef. As shown in Figure 10, higher CCN concentrations, total aerosol number concentrations, and CCN activation ratios were observed when air masses passed over the continent before reaching the reefs, despite them being less hygroscopic (susceptible to water absorption). This suggests that organic aerosols contribute significantly to CCN concentrations in the Great Barrier Reef region, highlighting the important role of inland emissions coming from Queensland. The air masses under continental influence exhibited higher total particle number concentrations (<math>631 \pm 209 \text{ cm}^{-3}</math>) compared to the marine influenced (<math>387 \pm 101 \text{ cm}^{-3}</math>), with a distinct bimodal aerosol size distribution observed during the marine periods, with an accumulation (&gt;60nm) and Aitken mode (&lt;60nm). In addition to total aerosol number concentration, the precipitation history along the back-trajectory also influenced CCN concentrations. These findings represent a first step toward developing a climatological understanding of aerosol and CCN properties over the Great Barrier Reef during summertime, a region and season where no prior observations have been reported. These findings have been published in the journal Atmospheric Chemistry and Physics (Horchler et al 2025).</p>  <p>Figure 10: CCN number concentration, hygroscopicity parameter <math>\kappa</math>, and CN number concentration for the marine periods MP (blue) and the continental periods CP (red) at 0.3 % SS. The black horizontal line in a box displays the median of the individual data. The lower and upper hinges represent the 25th and 75th percentiles. The upper and lower whiskers extend from the hinge to the largest or smallest measured values, respectively, but not more than 1.5 times the difference between the 25th and 75th percentiles. The mean is shown as grey points for the MP and grey triangles for the CP.</p> <p>Overall statistical analysis of all of the available observation data, from the GBR going back to 2016, reveals that particle number concentration is dominated by aerosol particles in the Aitken and accumulation mode and that CCN activation ratio</p>

Objective	Key Findings and/or Outcomes
	<p>remains overall fairly stable between years and seasons. Air masses are also overwhelmingly dominated by marine air masses, as evidenced by comparing the histogram of measured aerosol concentrations and continental influence (Figure 11). The most frequently measured values all coincide with no continental influence. Furthermore, CCN concentration correlates well with total particle number concentration Figure 11 (a) as well as different mode particle number concentrations, particularly accumulation mode Figure 11 (b). This suggests that the availability of aerosol particles is an important driver behind CCN concentration over the GBR, and the linear relationship between CCN and accumulation mode concentrations suggest accumulation mode concentrations as a good proxy for CCN concentration (Figure 11 (b)). A lack of correlation between CCN concentration and critical diameter suggests the chemical composition of the aerosol does not have a strong impact on overall CCN dynamics. This suggests it's likely that the chemical composition of particles that activate as CCN does not vary greatly. These hypotheses are furthermore strengthened by spatial analysis of data, showing that both CCN and total particle concentrations exhibit similar spatial behaviours, although at this stage spatial behaviour is difficult to quantify with the present dataset. The temporal analysis of CCN concentration and activation ratio implies that these parameters are not directly driven by solar radiation chemistry. Analysis of the aerosol number size distributions shows that although coral reefs appear to contribute to aerosol loading, their direct effect to CCN concentration appears to be minor - particularly in the bleaching season.</p> <div data-bbox="672 766 2016 1149"> <p>Figure 11 consists of three 2D histograms. The first plot, titled 'CCN vs N<sub>tot</sub>', shows CCN concentration (cm<sup>-3</sup>) on the y-axis (log scale from 10<sup>2</sup> to 10<sup>3</sup>) versus total particle number concentration (N<sub>tot</sub>, cm<sup>-3</sup>) on the x-axis (log scale from 10<sup>2</sup> to 10<sup>3</sup>). The frequency scale ranges from 0 to 200. The second plot, titled 'CCN vs N<sub>Acc</sub>', shows CCN concentration (cm<sup>-3</sup>) on the y-axis (log scale from 10<sup>2</sup> to 10<sup>3</sup>) versus accumulation mode particle number concentration (N<sub>Acc</sub>, cm<sup>-3</sup>) on the x-axis (log scale from 10<sup>2</sup> to 10<sup>3</sup>). The frequency scale ranges from 0 to 200. The third plot, titled 'Continental influence on CCN and N<sub>tot</sub>', shows CCN concentration (cm<sup>-3</sup>) on the y-axis (log scale from 10<sup>2</sup> to 10<sup>3</sup>) versus total particle number concentration (N<sub>tot</sub>, cm<sup>-3</sup>) on the x-axis (log scale from 10<sup>2</sup> to 10<sup>3</sup>). The color scale represents the median of land fraction, ranging from 0.0 (dark purple) to 0.6 (yellow).</p> </div> <p><i>Figure 11: Two-dimensional (2D) histograms of CCN and total particle number concentration and CCN and accumulation mode particle number concentration (a, b) and continental influence effect on CCN and total particle number concentration (c). The land fraction is calculated based on 72-hour HYSPLIT airmass back trajectories and presents the fraction of time the airmass was affected by continental or island emissions.</i></p> <p>Analysis of the aerosol dynamics over the reef suggests that fairly low aerosol and CCN concentrations and stable CCN activation ratio make MCB a viable intervention technique over the reef, because at lower aerosol loading it is easier to achieve meaningful albedo increase with MCB. Detailed understanding of spatial and temporal viability needs to be better characterised. Long-term continuous measurements will be required to capture the variety of atmospheric conditions more</p>

Objective	Key Findings and/or Outcomes
	<p>comprehensively over the entire latitudinal range of the sparsely observed GBR. This includes both transect voyages as well as stationary observations spanning several bleaching seasons. The dataset collected in the analysis can be used to support modelling studies that investigate this as well. Finally, CCN number concentrations can likely be predicted fairly reliably by simply measuring aerosol number concentrations above a certain size (~50 nanometre (nm)), meaning this can offer a more cost-effective method of acquiring spatial coverage of CCN concentrations over the reef.</p>
<p>10. Vertical profiles of the atmospheric boundary layer for meteorological (temperature, humidity) and aerosol (size distribution) properties.</p>	<p>All research flights conducted vertical profiles to map the thermodynamic structure of the atmosphere from the boundary layer through the trade winds layer (when present) into the free troposphere. Variability was observed. Furthermore, the marine boundary layer vertical extent was probed using simultaneous mini-Micropulse Lidar (MPL) measurements and meteorological observations on drones at One Tree Island (OTI) throughout February and March 2023 (Ryan et al. 2024). Good agreement was found in the boundary layer height retrievals from these two techniques despite Lidar being a remote sensing method and drones being a newly developed in-situ sampling method. Boundary layer heights above OTI were found to be remarkably stable throughout the campaign, between 700-900 metres altitude, with values in the morning typically slightly higher than in the afternoon.</p> <p>The vertical distribution of aerosol extinction was also explored at One Tree Island using the MPL, as well as a multi-axis differential optical absorption spectrometer (MAX-DOAS). MAX-DOAS retrieves aerosol extinction from oxygen absorption measurements and is most sensitive to the lowest 2 km of the atmosphere. Within this lower portion of the troposphere, good agreement in vertical aerosol distribution was found on average between the MPL and MAX-DOAS, with elevated aerosol layers around 1 km altitude frequently observed that are consistent with aircraft measurements in Braga et al. 2025. The polarisation capability of the MPL was also used to infer an increase in depolarisation ratio for aerosols above and below the boundary layer, which is consistent with the natural presence of sea salt aerosol layers already existing at altitudes around 1 km in the GBR environment (Ryan et al. 2024).</p> <p>The marine air masses over the GBR predominantly originated from the east to southeast and were transported by the trade winds (Braga et al. 2025). They exhibited a characteristic bimodal aerosol size distribution with relatively low concentrations (~ 200-300 cm<sup>-3</sup>) below cloud bases. Above cloud base, aerosol concentrations decreased with height, due to activation into cloud droplets and removal by cloud processes. High aerosol concentrations (~ 1000-1200 cm<sup>-3</sup>) were observed during episodes of continental outflow from eastern Australia. Boundary-layer transport was enhanced during periods of high-pressure advection over the region, while continental aerosols were frequently lofted into the free troposphere by convection and subsequently transported eastward toward the GBR by mid-tropospheric westerlies (~ 1-3 km) (Braga et al. 2025).</p>
<p>11. Analysis of the influence of meteorological and cloud microphysical processes on coral mass bleaching events.</p>	<p>The synoptic meteorology has a dominant role in defining the energy balance at the ocean surface, affecting not only incoming solar radiation, but also evaporative cooling (surface latent heat fluxes). When commonplace trade winds are present, the surface latent heat flux (cooling) prevents the GBR from overheating. When the trade winds break down, however, the evaporative cooling drops away and the ocean waters can heat up.</p> <p>The 2022 coral bleaching event, occurring under La Niña conditions, saw ocean temperatures at Davies Reef increase 1.9 °C over 19-days and subsequently cool 2.1 °C back to seasonal norms over eight days. This event was found to be triggered by</p>

Objective	Key Findings and/or Outcomes
	repeated Rossby wave breaking disrupting the local trade winds, thus inhibiting the latent heat flux. Latent heat fluxes, the primary driver of the event, tripled as the trade winds returned via rapid coastal ridging. These same synoptic features are concurrent with the historic Lismore flooding located hundreds of kilometres south of the GBR (Richards et al. 2024).

### Adjustments to key research objectives

Table 4: Variation in the Project over time.

Initial Research Question	Explain when, how and why the research question changed
No adjustments to report	

## 4 Future Research Recommendations

The atmospheric regime over the Great Barrier Reef is governed by a complex interaction of synoptic-scale weather systems, interannual climate oscillations such as the El Niño–Southern Oscillation (ENSO), and ongoing anthropogenic climate change. These drivers modulate cloud properties, surface irradiance, and ocean-atmosphere heat fluxes—factors that directly influence sea surface temperatures (SSTs) and the thermal stress experienced by coral reefs. As a result, a mechanistic understanding of atmospheric radiation dynamics, including aerosol-cloud interactions and feedback loops between SST anomalies and atmospheric convection, is fundamental to the optimisation of localised cooling and shading interventions such as marine cloud brightening (MCB) and fogging technologies.

The primary objective of the atmospheric survey and monitoring program is to characterise aerosol and cloud properties over the GBR to support the calibration and validation of atmospheric models and inform the development of intervention strategies. These models must be capable of capturing a wide range of meteorological conditions and climate phases to effectively guide the timing, scale, and location of potential interventions. In addition to their role in scenario testing, these models are essential for forecasting the short- and long-term implications of atmospheric interventions, not only on reef ecosystems but also on adjacent coastal and atmospheric systems.

Model-informed deployment of MCB will require spatial prioritisation, as operational, economic, and energy constraints may prevent implementation across the entire reef. Effective targeting depends on identifying both the area's most at risk of thermal stress and the regions where interventions are likely to be most effective. This, in turn, necessitates a strong understanding of the background atmospheric state, particularly with regard to CCN concentrations. Enhancing cloud albedo through MCB depends on introducing cloud-seeding aerosols into an environment where background CCN levels are responsive to yield measurable increases in cloud droplet number and brightness. Quantifying the spatial variability and baseline concentrations of marine aerosols across the GBR is therefore, a prerequisite for determining the particle injection thresholds required to generate a meaningful brightening response.

Recognising the importance of atmospheric composition in shaping the effectiveness of cooling interventions, there is a clear need for sustained, long-term atmospheric monitoring across the GBR. While the restoration research community has invested heavily in long-term monitoring of ocean conditions and coral life histories, comparable effort must now be directed toward understanding atmospheric dynamics. In particular, continuous measurements of CCN concentrations and their variability over seasonal to interannual timescales are essential for both operational planning and long-term impact assessments.

Findings from the RRAP GBR Atmospheric Survey Project (CS-01) and the Atmospheric and Meteorological Monitoring Project (CS-02) have demonstrated that short-term monitoring from mobile research platforms, such as vessels operating over a few weeks, is insufficient to capture the full spatial and temporal variability of aerosol and CCN distributions in the GBR. Although vessels can carry comprehensive instrumentation, their use for dedicated atmospheric monitoring is cost-prohibitive and operationally constrained. Piggybacking on other RRAP voyages presents additional challenges, including contamination of air samples from ship exhaust and logistical difficulties in maintaining suitable upwind trajectories for data collection. Furthermore, the use of research vessels in different locations across different years introduces significant uncertainty, making it difficult to separate long-term trends from spatial variability in the atmospheric data. Ship-based measurements also require a trained operator, which adds resource demands that are difficult to justify for routine monitoring.

To address these limitations and progress toward a more robust monitoring framework, a revised strategy is required. Intensive, long-duration campaigns in fixed locations, such as Heron Island, should continue to provide high-quality data capable of disentangling spatial from temporal aerosol variability. These data are essential for improving our understanding of seasonal CCN dynamics, particularly during coral bleaching periods. Concentrated efforts at a single site allow researchers to track aerosol properties over time, identify processes driving CCN fluctuations, and assess the long-term influence of both natural variability and

potential interventions. Such detailed observational records are also crucial for the validation of atmospheric models and simulations used in intervention planning.

In parallel, the feasibility of deploying a broader network of low-cost, low-power particle counters across the GBR should be explored. These instruments could be integrated into existing infrastructure, such as AIMS weather stations or at research stations, to provide a geographically distributed view of CCN concentrations across the reef. Establishing this kind of observational network would support characterisation of spatial gradients in aerosol properties, help detect shifts in the atmospheric background over time, and enhance situational awareness during future intervention trials. Because CCN availability appears to be most strongly linked to the presence of sufficiently large aerosol particles, even relatively simple instruments could yield valuable data if deployed strategically. Several candidate sensors are currently under evaluation for long-term use in the reef environment, and a coordinated assessment of their suitability should be prioritised.

Together, these recommendations point to a necessary transition from short-term, campaign-based aerosol monitoring toward a regionally distributed, long-term observational system tailored to the specific needs of climate intervention research. By strengthening the atmospheric data foundation that underpins MCB and fogging technologies, RRAP can advance the development of operationally feasible and scientifically robust strategies to reduce bleaching risk and support the resilience of the GBR in a warming climate.



*Figure 12: High and low cloud visible at sunset over the Great Barrier Reef*

## 5 References

- Braga, R. C., Rosenfeld, D., Hernandez, D., Medcraft, C., Efrain, A., Moser, M., Lucke, J., Doss, A., & Harrison, D. (2025). Cloud processing dominates the vertical profiles of aerosols in marine air masses over the Great Barrier Reef. *Atmospheric Research*, 315, 107928. <https://doi.org/10.1016/j.atmosres.2025.107928>.
- Horchler, E. J., Alroe, J., Harrison, L., Cravigan, L., Harrison, D. P., and Ristovski, Z. D.: Measurement report: Aerosol and cloud nuclei properties along the Central and Northern Great Barrier Reef – impact of continental emissions, *Atmos. Chem. Phys.*, 25, 10075–10087, <https://doi.org/10.5194/acp-25-10075-2025>, 2025
- Hillger D, Seaman C, Liang C, Miller S, Lindsey D, Kopp T (2014) Suomi NPP VIIRS Imagery evaluation. *J Geophys Res Atmos* 119:6440-6455. <https://doi.org/10.1002/2013JD021170>
- Hillger D, Kopp T, Lee T, Lindsey D, Seaman C, Miller S, Solbrig J, Kidder S, Bachmeier S, Jasmin T, Rink T (2013) First-Light Imagery from Suomi NPP VIIRS. *Bull Am Meteorol Soc* 94:1019-1029. <https://doi.org/10.1175/BAMS-D-12-00097.1>
- Okuljar, M., Sulo, J., Horchler, J., Alroe, J., Li, Z., Miljevic, B., Harrison, D., & Ristovski, Z. (2025). Measurement report: Aerosol chemical composition in the Great Barrier Reef region during summer. Manuscript submitted for publication in *Atmospheric Chemistry and Physics Discussions*.
- Richards, L.S., Siems, S.T., Huang, Y. Zhao, W., Harrison, D., Manton, M. & Reeder, J. The meteorological drivers of mass coral bleaching on the central Great Barrier Reef during the 2022 La Niña. *Sci Rep* 14, 23867 (2024). <https://doi.org/10.1038/s41598-024-74181-2>
- Richards LS, Siems ST, Huang Y, Zhao W, Harrison DP, Manton MJ, Reeder MJ (2024) The meteorological drivers of mass coral bleaching on the central Great Barrier Reef during the 2022 La Niña. *Sci Rep* 14:23867. 10.1038/s41598-024-74181-2
- Rosenfeld D, Zhu Y, Wang M, Zheng Y, Goren T, Yu S (2019) Aerosol-driven droplet concentrations dominate coverage and water of oceanic low-level clouds. *Science* 363:eaav0566. 10.1126/science.aav0566
- Rosenfeld D, Zheng Y, Hashimshoni E, Pöhlker ML, Jefferson A, Pöhlker C, Yu X, Zhu Y, Liu G, Yue Z, Fischman B, Li Z, Giguzin D, Goren T, Artaxo P, Barbosa HMJ, Pöschl U, Andreae MO (2016) Satellite retrieval of cloud condensation nuclei concentrations by using clouds as CCN chambers. *Proceedings of the National Academy of Sciences* 113:5828-5834. doi:10.1073/pnas.1514044113
- Ryan Robert G., Eckert Christian, Kelaher Brendan P., Harrison Daniel P., Schofield Robyn (2024) Boundary layer height above the Great Barrier Reef studied using drone and Mini-Micropulse LiDAR measurements. *Journal of Southern Hemisphere Earth Systems Science* 74, ES24008.
- Ryan RG, Toms-Hardman L, Smirnov A, Harrison DP, Schofield R (2025) Measurement report: Aerosol vertical profiling over the Southern Great Barrier Reef using lidar and MAX-DOAS measurements. *Atmos Chem Phys* 25:11183-11197. 10.5194/acp-25-11183-2025
- Zhao W, Huang Y, Siems S, Manton M (2022) A characterization of clouds over the Great Barrier Reef and the role of local forcing. *International Journal of Climatology*. <https://doi.org/10.1002/joc.7660>

